



# The elastic deformability and strength of a high porosity, anisotropic chalk

M.L. Talesnick<sup>a,\*</sup>, Y.H. Hatzor<sup>b</sup>, M. Tsesarsky<sup>b</sup>

<sup>a</sup>Faculty of Civil Engineering, Technion–Israel Institute of Technology, Haifa, Israel

<sup>b</sup>Department of Geological and Environmental Sciences, Ben Gurion University of the Negev, Be'er Sheva, Israel

Accepted 9 April 2001

## Abstract

The submission explores the mechanical behavior of a very porous chalk formation, in which a system of ancient caverns was excavated. Incidents of general and localized failure of these ancient caverns initiated a comprehensive laboratory testing program aimed at investigating the anisotropic nature of the stress–strain response and strength of the material. It was felt that these aspects could be of profound importance in the stability of the cavern systems. The effect of water content over a broad range from 1.5% to saturation, on the compressive and tensile strength was also studied. Testing was based on the hollow cylinder methodology and was supplemented with uniaxial compression of solid cylinders and diametric compression of Brazilian disks. Use of the hollow cylinder methodology was extended to failure conditions.

Test results illustrate the anisotropic nature of the stress–strain response of the chalk. The material clearly displays transverse isotropy, with horizontal bedding planes corresponding to the plane of material symmetry. The modulus of deformation within the plane of material symmetry is significantly higher than that perpendicular to bedding planes. Torsional shear of hollow cylinder specimens was employed to measure the shear modulus of the chalk.

The testing carried out up to failure illustrated the anisotropy of the chalk strength. The compressive strength was found to be 50% higher in compression parallel to bedding than perpendicular to bedding. Increasing water content was found to have a consistent detrimental effect on compressive strength, tensile strength and material stiffness. The most drastic effect was found due to relatively small increases in water content, at initial water contents of less than 5%. Anisotropy of the chalk strength was found to persist over the entire range of water contents considered. © 2001 Elsevier Science Ltd. All rights reserved.

*Keywords:* Chalk; Anisotropy; Laboratory testing; Elasticity; Strength; Water content; Hollow cylinder testing

## 1. Introduction

The bell-shaped caverns of Beit Guvrin in central Israel have been subject to unstable structural behavior. More than 800 caverns are found in the Beit Guvrin area, many of which are within the jurisdiction of the Beit Guvrin National Park. The caverns form an integral part of a historic site, which serves today as an out of doors archeological museum visited by more than 200,000 tourists per year.

In 1996/1997 the National Parks Authority of Israel initiated a study of the stability of the caverns in order

to evaluate the dangers of ongoing usage and development of the site as a tourist attraction. The overall thrust of the study was to evaluate which caverns or cavern sections should be left accessible to the public and which sections would require some form of remedial support such that the public could use the park safely. Results of stability analyses and in-situ monitoring are presented by Tsesarsky [1] and Tsesarsky, Hatzor and Talesnick [2].

The caverns were carved approximately 1400 years ago in the soft chalk of the Marasha formation. Little significant data concerning the mechanical behavior of such lithologies is available in the engineering literature. An extensive testing program was carried out in order to provide the required input data for the stability analyses.

\*Corresponding author.

E-mail address: talesnick@tx.technion.ac.il (M.L. Talesnick).

The objective of the current submission is to describe the stress–strain behavior and strength characteristics of the high porosity chalk in which the caverns are found. Significant effort has been placed on describing the effect of changes in water content on compressive strength and on the anisotropy of compressive strength.

### 1.1. General and historical background

The bell caverns of Beit Guvrin were excavated from the early seventh century through the 11th century [3]. The caverns were originally excavated to provide a source of building stone. The material was most likely chosen for its ease of excavation and shaping rather than for its durability. In later years, the caverns were used as storage facilities, sites for performing ceremonial rituals, and at times served as dwellings. The caverns were formed by excavating a 0.6–0.9 m diameter shaft through the calcareous caliche crust (locally known as Nari). The thickness of the Nari crust typically extends from the ground surface to a depth of between 1.5 and 2.5 m (Fig. 1). Upon passing through the harder caliche crust the shaft was increasingly widened out with depth, and the soft chalk below was quarried. Single caverns reach heights of up to 18 m and a base diameter of up to 20 m. As the quarrying operations advanced, the spacing between adjacent caverns was reduced and eventually cavern volumes overlapped, creating groups of large multiple domed openings (Fig. 2), supported by irregularly spaced and shaped ribs and pillars. Over the years, many of the openings have collapsed, creating large courtyards with near vertical boundaries. Within the courtyards, remains of the caliche crust and chalk boulders are found lying on the ground (Fig. 3). Many of the caverns and cavern complexes are currently at different stages of structural collapse. In fact, two significant failures occurred over the past five years and shear luck was the only reason that loss of life did not occur.



Fig. 1. Nari crust interface.



Fig. 2. Set of caverns with overlapping volumes, the width of the caverns varies between 20–25 m.



Fig. 3. Courtyard boundary, Nari and chalk remains.

All the known bell caverns of the area were excavated in an Eocene chalk of the Marasha Formation. The chinks of the Beit Guvrin area are generally massive, uniform, very soft and of extremely low dry density. Layers are relatively thick. The area of the archeological digs is crossed by three very widely spaced sub-vertical joint sets, and one very persistent bedding plane. Due to the fact that joint spacing is quite large, problems of rock block failure in singular caverns are limited, however block failures are noted in overlapping caverns. Dry unit weight varies between 10.7 and 11.1 kN/m<sup>3</sup>, which translates to a porosity of approximately 60% (for  $G_s = 2.70$ ). Chinks of the Eocene are widespread in Israel; at many locations the Marasha chalk is found at the ground surface, or relatively close to ground surface. Because of its soft nature and ease of excavation the chinks of the Marasha formation have been utilized throughout history as host rock for underground openings. The same is true at present; several contemporary underground projects in Israel have recently been completed in Eocene chinks. Some projects were

excavated in the Marasha formation, while others were constructed in different formations, in chalks of similar nature. The overall massive character of the formation makes the properties of the intact rock important in the investigation of the stability of the openings. It is surprising that only minimal information is available concerning the fundamental mechanical response of these rocks.

### 1.2. Background literature

Since the mid-1980s considerable research effort has been aimed at quantifying and modeling the behavior of high porosity chalks. Much of the data has been taken from drained and undrained triaxial compression testing performed under a variety of stress paths. Test results have been published by many researchers (e.g. [4–7]). These results have been used in the development of numerical models aimed at simulating the compaction of North Sea chalks due to pore pressure reduction and shear stress increase (e.g. [8]). All the models are based on large strain plastic behavior, and to some extent founded on the principles of soil mechanics, in particular, critical state soil mechanics.

The geotechnical properties of different chalks have been investigated by a considerable number of researchers (e.g. [10–13]). The geotechnical properties of several Israeli chalks have been considered by Hayati [14], Flexer et al. [15] and Polishook [16]. The majority of these publications describe different correlations between material parameters such as dry density (porosity), unconfined compression strength (dry and saturated), Brazilian tensile strength, sonic velocity, carbonate content and deformation moduli for different chalk formations. Many of the studies have focused on correlations between dry density (porosity) and strength, either compressive or tensile (e.g. [9,10,14,16]). Several studies have, in a limited way, attempted to consider anisotropy of strength and deformation characteristics of chalks by testing specimens oriented in various directions to bedding planes [17,10,13]. Results obtained were not conclusive, in part due to limited testing and variability of the test results.

Two important aspects of material behavior have not been adequately addressed in the literature: (I) The small strain “elastic” behavior of chalks, in particular of high porosity chalks, and (II) the influence of variation in water content on the strength, stiffness and “elastic” response of high porosity chalks.

Studies considering the small strain behavior of chalks have been limited to simple stress conditions of uniaxial or triaxial compression. In comparing small strain laboratory data to field interpreted data, Mathews and Clayton [18] and Clayton et al. [19] assumed isotropic material behavior. Jardine et al. [17] presented limited data which illustrated isotropy of the modulus of

deformation based on triaxial compression testing of two mutually perpendicular oriented specimens. Talesnick and Brafman [20] presented some initial data on the non-linear and anisotropic stress–strain nature of two Israeli chalks. Tests on intact laboratory specimens indicated highly non-linear stress–strain response. The material stiffness was shown to decline by up to 30% as strains reached a magnitude of  $1500\ \mu\epsilon$ . Significant anisotropy of material stiffness parallel and perpendicular to the direction of sedimentation was observed. The initial material stiffness was shown to be 50% higher when measured in a direction perpendicular to the direction of sedimentation, compared to that measured parallel to the direction of sedimentation. The general stress–strain behavior of chalk in the small strain range has not been the focus of published research. To be specific, isotropy, linearity and the response of chalks to varied stress conditions has not been widely considered. The importance of integrating anisotropy and non-linearity into practical, material models has been illustrated to be of significant general engineering importance by Amadei [21], and of specific importance with respect to chalks by Burland [22] and Jones et al. [23].

The detrimental effect of water on the strength of chalk has been demonstrated in several publications. Bell [24], Hayati [14], Mortimore and Fielding [9] among others, have all shown that the uniaxial compressive strength of chalks is significantly reduced when tested under saturated conditions. Bell et al. [10] and Hayati [14] illustrated that this observation is true for a wide range of porosities, and that the higher the porosity, the greater the reduction of strength with saturation. Hayati [14] and Mathews and Clayton [18] noted that material stiffness follows a similar trend with saturation. Several researchers have suggested that the reduction in both strength and stiffness may be linked, in part, to the dissipation of suctions due to inundation of fluid, together with chemical processes which occur upon saturation. Despite the indisputable effect of water on the strength of unsaturated chalks, only limited data linking distinct variations of compressive strength, tensile strength and stiffness of chalks with water content is found in the literature. Furthermore, study of the effect of variations in water content on the isotropy of strength and stiffness of chalks is notably absent from the professional and academic literature.

## 2. Experimental approach and testing program

The scope of the experimental program included testing for the investigation of both stress–strain and strength characteristics of the Marasha chalk. The program was based on different laboratory testing procedures, including testing of hollow cylinders,

uniaxial compression of solid cylinders and diametrical compression of Brazilian disks. A substantial part of the testing program was based on the hollow cylinder testing methodology described by Talesnick et al. [25] and extended by Talesnick and Ringel [26] and Talesnick et al. [27]. The idea behind the hollow cylinder methodology is that a single hollow cylindrical specimen may be tested several times, each time under different stress conditions. From the material response to each individual stress condition, a set of different material stress–strain parameters may be determined. This situation is advantageous since inter-specimen variations in material properties are eliminated. In determining elastic stress–strain characteristics, the methodology imposes three significant restrictions:

(I) The strains incurred due to the application of each individual stress condition must be fully recoverable. This restriction is important since it assures that the application of earlier stress conditions do not change the material which in turn would lead to variations in the material stress–strain response to subsequent stress conditions.

(II) Only material which displays transverse isotropy or complete isotropy may be considered.

(III) The axis of material symmetry must coincide with the axis of geometric symmetry. In the case of most sedimentary deposits, the direction of sedimentation may be initially assumed to be parallel to the axis of material isotropy.

For an elastic solid displaying transverse isotropic behavior the relationship between stresses and strains (or their increments) may be expressed as shown:

$$\begin{bmatrix} \varepsilon_z \\ \varepsilon_\theta \\ \varepsilon_r \\ \gamma_{\theta z} \\ \gamma_{rz} \\ \gamma_{\theta r} \end{bmatrix} = \begin{bmatrix} \frac{1}{E'} & & & & & \\ \frac{v'}{E'} & \frac{1}{E} & & & & \\ & \frac{v}{E} & \frac{1}{E} & & & \\ -\frac{v'}{E'} & -\frac{v}{E} & & & & \\ 0 & 0 & 0 & \frac{1}{G'} & & \\ 0 & 0 & 0 & 0 & \frac{1}{G'} & \\ 0 & 0 & 0 & 0 & 0 & \frac{1}{G'} \end{bmatrix} \begin{bmatrix} \sigma_z \\ \sigma_\theta \\ \sigma_r \\ \tau_{\theta z} \\ \tau_{rz} \\ \tau_{\theta r} \end{bmatrix}, \quad (1)$$

where

$$\begin{aligned} E' &= E_z, & v' &= v_{\theta z} = v_{rz}, \\ E &= E_{rr} = E_{\theta\theta}, & v &= v_{r\theta} = v_{\theta r}, \\ G' &= G_{\theta z} = G_{rz}, & G &= \frac{E_{\theta\theta}}{2 \cdot (1 + v_{\theta r})}. \end{aligned}$$

Eq. (1) has been written in cylindrical coordinates, where the  $\theta r$  plane coincides with the plane of material isotropy (see Fig. 4). The coefficient matrix of Eq. (1) is symmetrical.  $E'$  and  $v'$  represent the modulus of

deformation and the Poisson ratio perpendicular to the plane of material isotropy respectively.  $E'$  and  $v'$  represent the same parameters within the plane of material isotropy.  $G'$  is the shear modulus in planes perpendicular to the plane of material isotropy.

The nomenclature employed in the hollow cylinder methodology is illustrated schematically in Fig. 4. For a transversely isotropic solid, three different conditions of stress must be applied to a hollow cylinder specimen in order to define the “elastic” stress–strain response of the material. Uniaxial compression tests (application of  $\sigma_z$  alone) allow the determination of the required parameters perpendicular to the plane of material isotropy,  $E'$  and  $v'$ . Radial compression tests (application of  $\sigma_{r0}$  alone) allow the determination of the stress–strain properties within the plane of material isotropy,  $E$  and  $v$ . Hollow cylinder torsion (application of a moment  $\mathbf{T}$ ) is employed for the determination of the shear modulus  $G'$ . The analytical expressions for the determination of the material parameters from the different testing configurations are presented in full by Talesnick and Ringel [26] and Talesnick et al. [27].

It should be noted that the stress–strain response of the rock may not be identical under compression and tension. The parameters  $E'$ ,  $E$ ,  $v'$  and  $v$  may require determination both in the compressive and tensile stress regimes. Talesnick and Brafman [20] and Talesnick et al. [27] illustrated how these parameters can be evaluated when the material is subjected to tension.

In the present study, the overall stress–strain response of the Marasha chalk has been investigated under air-dried conditions alone. Results of tests performed on air-dried hollow cylinder specimens under conditions of uniaxial compression, radial compression and torsional shear are presented and analyzed. The effect of water content on the stress–strain response of the chalk, has been for technical reasons limited to radial compression testing. The degree of material stress–strain anisotropy has been evaluated based on the magnitudes of the different moduli of deformation as determined from the different testing configurations. The anisotropy reflected in Poisson’s ratio is not discussed here.

Hollow cylinder testing was supplemented by diametric compression of Brazilian disks and uniaxial compression of solid cylinders oriented both parallel and perpendicular to the plane of material isotropy. Both of these additional techniques can be employed in determining the five material parameters of Eq. (1). However, in both testing configurations, multiple specimens must be tested for complete determination. Diametric compression of Brazilian specimens to study the anisotropy of the elastic response of rock was first proposed by Hondros [28]. An advantage of implementing the diametric compression test is that both the elastic moduli and the tensile strength may be determined from a single, simple test. Talesnick and Bloch-Friedman [29]

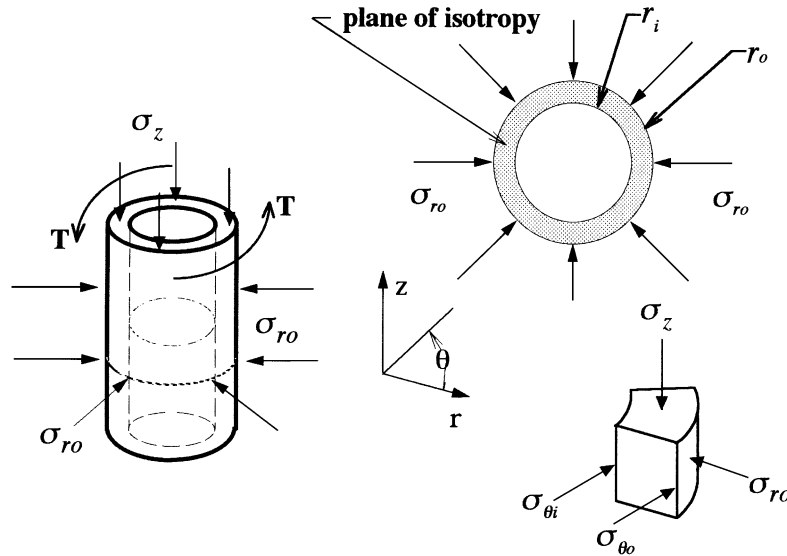


Fig. 4. Coordinate system, nomenclature and stress conditions used in the hollow cylinder testing methodology.

and Talesnick et al. [27] illustrated that the elastic stress–strain parameters determined by employing the hollow cylinder methodology compare extremely well with those determined through uniaxial and diametrical compression.

Investigation of the strength characteristics of the chalk was performed within a framework of three inter-related objectives: (I) To consider the isotropy of the chalk compressive strength when loaded in directions perpendicular and parallel to the axis of sedimentation, (II) to consider the effect of water content on the strength characteristics of the chalk, and (III) to experimentally consider the validity of employing radial compression tests in the investigation of strength anisotropy.

Strength testing included failure of hollow cylinder specimens in uniaxial and radial compression, uniaxial compression of oriented solid cylinders and diametrical compression of Brazilian disks.

Compressive strengths were determined from the peak stresses of the resulting stress–strain plots. Results of the uniaxial compression tests (whether performed on hollow cylinder specimens or solid cylinders) represent the unconfined compressive strength of the material in the direction of the applied stress. In the present study, testing was performed on specimens oriented either perpendicular or parallel to the direction of sedimentation.

Radial compression testing of hollow cylinder specimens induces a gradient of tangential stress across the specimen wall. The maximum tangential compressive stress develops at the inner specimen diameter ( $\sigma_{\theta i}$ ). When outer pressure of sufficient magnitude is applied, compressive failure of the specimen wall ensues. For cases where the  $\theta r$  plane of the hollow cylinder specimen

is aligned with the plane of sedimentation, the compressive strength parallel to the plane of sedimentation may be determined according to [30]

$$\sigma_{\theta i, f} = 2 \cdot \sigma_{r o, f} \cdot \frac{r_o^2}{r_o^2 - r_i^2}, \tag{2}$$

where  $\sigma_{\theta i, f}$  is the applied outer radial pressure at the onset of failure.

It may be argued that due to the non-uniformity of both the radial and tangential stresses across the specimen wall, the strength obtained from radial compression testing may not be a true representation of uniaxial compression strength. Santarelli and Brown [31] have presented data which suggest that compressive strengths based on radial compression of hollow cylinders as determined from Eq. (2) are significantly higher than those measured in standard uniaxial compression tests. The experimental validity of compression strengths as based on Eq. (2) will be considered by comparing results from radial compression tests to those determined from uniaxial compression of suitably oriented cylindrical specimens.

Tensile strength of the Marasha chalk has been based upon the results of diametrical compression of Brazilian disks. The tensile strength is determined based on Eq. (3).

$$\sigma_{t, Braz} = \frac{2 \cdot P_f}{\pi \cdot d \cdot t}, \tag{3}$$

where  $d$  is the specimen diameter,  $t$  is specimen thickness and  $P_f$  is the compressive load at failure.

The effect of water content on the strength of the chalk was investigated by bringing specimens to predetermined water contents, and subsequent testing under different experimental configurations. The effects

of water content on strength, isotropy and stress–strain response were each considered.

### 3. Preparation and instrumentation of specimens

All the test specimens were prepared from a series of 15, 150 mm diameter cores which were extracted from the ground surface next to the entrance of a bell cavern in advanced stages of failure. The cores were drilled vertically, perpendicular to the apparent bedding planes. The material sampled was typical of the virgin, undisturbed chalk.

Hollow cylinder specimens were prepared by first drilling a solid cylinder of nominal diameter 31.4 mm, parallel to the direction of coring of the original 150 mm diameter core. The cylindrical void was then overcored by exchanging diamond bits without disturbing the alignment of the vertical axis. This preparation procedure yields hollow cylinder specimens of nominal inner and outer diameters of 38.1 and 53.3 mm, respectively, and a solid (inner core) cylindrical specimen of 31.4 mm diameter. Typical lengths of hollow cylinder specimens ranged from 85 to 110 mm, while inner core cylinders were typically shortened to between 75 and 80 mm. The specimen ends were ground flat and parallel by means of a diamond wheel mounted on a surface grinder. The fact that two specimens are created from within the same volume of material is advantageous since it reduces material variability to a minimum.

Brazilian disks were prepared by coring 53.3 mm diameter specimens perpendicular to bedding planes. The specimen ends were ground such that typical disk thickness ranged between 25 and 35 mm.

Following preparation, all specimens were dried to a constant mass at a temperature of 40°C. Based on the specimen mass and dimensions at 40°C, a dry density for each specimen was estimated. The dry unit weight ( $\gamma_d$ ) of all the specimens fell within the range of 10.7–11.1 kN/m<sup>3</sup>. Each specimen, except for those tested at air dried conditions was brought to a specific, predetermined total mass by placing water saturated filter paper strips in contact with the specimen. The specimen was then placed in a plastic, zip lock bag, which in turn was placed in a desiccator. The total mass of each specimen was measured on a daily basis. Water saturated filter strips were reapplied to the specimen until the target mass was achieved. Specimens were then allowed to cure over a 2-week period while stored in separate plastic bags within the desiccator. Specimens tested under “saturated” conditions were brought to this state by submerging the entire specimen until the measured (surface dry) total mass stabilized. The specimens did not reach complete saturation, but rather approached a degree of saturation of 84%, at a water content of approximately 47%.

All water contents reported in the following sections are those measured after the completion of the testing procedure, and are based on measured dry mass following 24 h at 105°C.

Strains were measured by one of two methods. Hollow cylinder specimens tested at air-dry conditions were instrumented with four pairs of strain gages. Each pair was strategically placed (Fig. 5a) in order to follow the development of axial strain ( $\epsilon_z$ ), inner tangential strain ( $\epsilon_{\theta i}$ ), outer tangential strain ( $\epsilon_{\theta o}$ ) and outer shear strain ( $\gamma_o$ ). Air-dried Brazilian disks were instrumented with a pair of mutually perpendicular stacked strain gages affixed at the specimen center (Fig. 5b). The bonding process for all specimen configurations, and the capabilities of the strain measurement system are described by Talesnick et al. [27].

Use of bonded strain gages on specimens brought to water contents of 6–7% and higher, proved to be problematic. Two basic difficulties became apparent: (I) the strain gage which acts as a resistor, warms the immediate vicinity, causing local changes in water content, introducing drift into the output strain readings, (II) bonding between the softer, wet chalk and the strain gage becomes tenuous at water contents greater than 5–6%. For this reason, strain measurements in specimens tested with water contents greater than 5% were performed with specially manufactured clip gages.

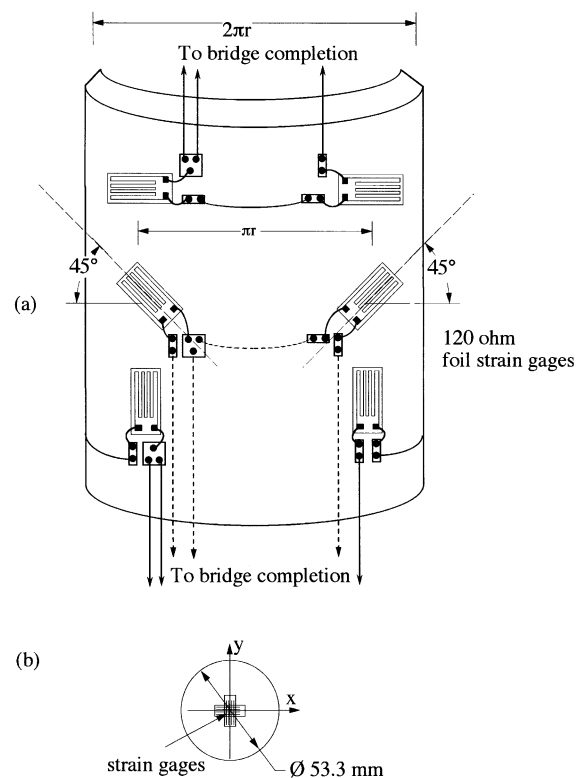


Fig. 5. Strain gage configuration on test specimens: (a) hollow cylinder specimens, and (b) Brazilian test specimens.

These clip gages are carefully designed, strain gage based deflection transducers, capable of resolving deformations on the order of 0.5  $\mu\text{m}$ . Obviously, there exists a balance between resolution and system compliance, relative to the specimen stiffness. The clip gages were used to measure changes in the outer diameter of hollow and solid cylinder specimens; and changes in inner diameter of hollow cylinder specimens. Clip gages for the measurement of axial deformations in soft, wet material are in advanced stages of development.

#### 4. Results and discussion

##### 4.1. Anisotropic stress–strain response and compressive strength

Characteristic stress–strain response of the air-dry Marasha chalk at Beit Guvrin is presented in Figs. 6–11. Fig. 6a presents the stress–strain response of two hollow cylinder specimens loaded in uniaxial compression. Specimen BGHC4 was loaded under strain controlled conditions to failure, which occurred at an axial stress ( $\sigma_z$ ) of 5.95 MPa and a corresponding axial strain ( $\epsilon_z$ ) of 5000  $\mu\epsilon$ . The second specimen (BGHC1) was loaded under stress controlled conditions to an axial stress of 2.7 MPa and subsequently unloaded. Both specimens illustrate similar non-linearity in their stress–strain response. The stress–strain data shown in Fig. 6a is typical of the material response to stresses applied perpendicular to bedding planes. Fig. 6b presents the

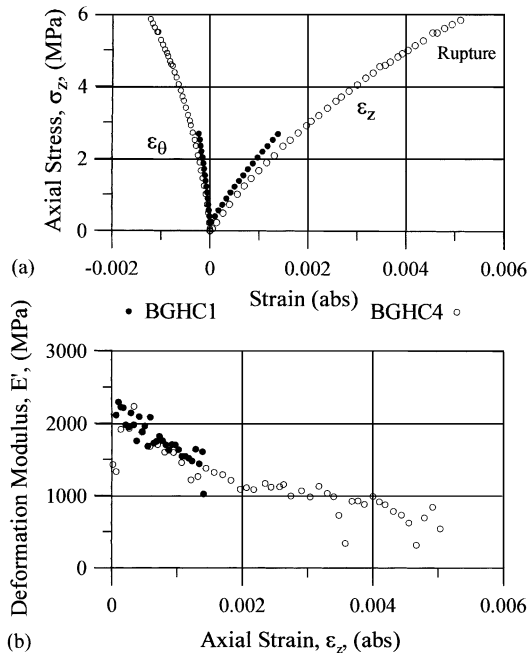


Fig. 6. Results of uniaxial compression testing: (a) stress–strain response, and (b) variation in modulus of deformation  $E'$ .

instantaneous magnitude of the modulus of deformation ( $E'$ ) as a function of increasing axial strain. The figure clearly illustrates the continuous decrease in stiffness from the onset of loading. The initial magnitude of  $E'$  is approximately 2300 MPa. The absence of an initial linear zone is very definite. The rate of change in  $E'$  is rapid at small axial strains, however it moderates and becoming almost uniform at a rate of 0.225 MPa/ $\mu\epsilon$  at strains of greater than 2000  $\mu\epsilon$ .

Fig. 7a presents typical stress–strain response of a pair of hollow cylinder specimens subjected to radial compression. The plots represent the material response to stress applied within (or parallel) to bedding planes. Specimen BGHC3 was loaded to failure, which occurred at an outer radial pressure ( $\sigma_{ro}$ ) of 2.4 MPa. According to Eq. (2), this corresponds to an inner tangential compressive stress ( $\sigma_{\theta i}$ ) of 9.6 MPa. The specimen failed when the inner tangential strain ( $\epsilon_{\theta i}$ ) was 4500  $\mu\epsilon$ . The second specimen (BGHC1) was loaded to a predefined outer pressure of 0.9 MPa and subsequently unloaded. Both specimens display definite and continuous non-linearity in their stress–strain response, from the very outset of pressure application. Changes in the instantaneous magnitude of the modulus of deformation ( $E$ ) for both specimens is plotted in Fig. 7b. The initial modulus of deformation parallel to the bedding planes is approximately 4500 MPa.

The response of the chalk to radial compression is generally similar to that observed in uniaxial compression. The material displays highly non-linear behavior. No linear zone is apparent. The modulus of deformation,  $E$ , decreases rapidly until an inner tangential

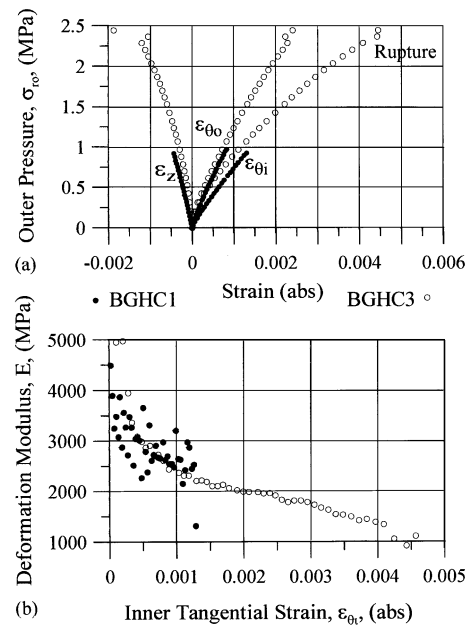


Fig. 7. Results of radial compression testing: (a) stress–strain response, and (b) variation in modulus of deformation  $E$ .

strain ( $\varepsilon_{\theta i}$ ) of  $1500 \mu\epsilon$  is reached. At strains larger than  $1500 \mu\epsilon$  the rate of change becomes uniform at a value of approximately  $0.355 \text{ MPa}/\mu\epsilon$ . The strains measured at failure are close in magnitude to those recorded in uniaxial compression.

Despite the similarities in the general stress–strain response, the data presented in Figs. 6 and 7 accentuate two important aspects of the anisotropic nature of the mechanical response of this chalk:

(I) The initial value of  $E$  ( $\sim 4500 \text{ MPa}$ ) determined from radial compression testing is significantly higher than  $E'$  ( $\sim 2300 \text{ MPa}$ ) determined from uniaxial compression tests. Table 1 presents values of  $E$  and  $E'$  at different levels of strain. The ratio  $E/E'$  illustrates the anisotropy of material stiffness over a wide range of strain. There is no doubt that the material stiffness parallel to bedding is greater than that perpendicular to bedding. It may also be seen that the ratio of the moduli of deformation remains relatively constant at strains levels greater than  $1000 \mu\epsilon$ .

(II) The stress required to induce compressive failure parallel to bedding is significantly different from that perpendicular to bedding. Three air-dried hollow cylinder specimens were brought to failure in uniaxial compression. Failure occurred at axial stresses ( $\sigma_z$ ) of 5.5, 5.95 and 6.2 MPa. Two air-dried hollow cylinder specimens were brought to failure in radial compression. Failure occurred when inner tangential stresses ( $\sigma_{\theta i}$ ) reached 9.3 and 9.6 MPa. Based on simple arithmetic averages, the ratio of the compressive strength parallel to bedding to the compressive strength perpendicular to bedding is  $(9.45/5.9)$  1.60, which is surprisingly close to the ratio  $E/E'$  shown in Table 1 for strain levels greater than  $1000 \mu\epsilon$ . In a manner similar to the stress–strain response, the strength of the chalk is significantly greater parallel to bedding than perpendicular to bedding.

As noted earlier, Santarelli and Brown [31] have suggested that failure of hollow cylinder specimens in radial compression may not be a suitable representation of the uniaxial compressive strength in the  $\theta r$  plane. It is debatable whether the condition of stress at the inner fiber of a hollow cylinder specimen subjected to radial compression is actually one of uniaxial compression. However, a basis by which results of radial compression tests may be used as a measure of compressive strength may be established by comparing uniaxial compressive strengths of specimens cored parallel to bedding to that

of radial compressive strengths of specimens cored perpendicular to bedding.

Tsesarsky [1] performed a series of triaxial and uniaxial compression tests on specimens from the same series of cores drilled at Beit Guvrin. Three uniaxial compression tests were performed on solid cylindrical specimens prepared with their axes parallel to bedding. He reported uniaxial compression strengths of 8.4, 9.1 and 12.5 MPa. The scatter of the results is somewhat larger than that of the radial compressive strengths, however, the average value of 10 MPa compares very well to that of 9.5 determined in radial compression testing.

Based on the available data, the radial compression test provides a suitable means for evaluating the compressive strength of a material, provided that the  $\theta r$  plane is a plane of material isotropy. This assumption will be implemented when considering the effect of water content on compressive strength.

#### 4.2. Response to pure shear

Fig. 8 presents data recorded during a single load–unload cycle of torsional shear applied to a hollow cylinder specimen. While it may not be obvious from the plot, it will be demonstrated that the shear stress–shear strain response is inherently non-linear. Upon removal of the shear stress hysteresis of the shear strain develops. Despite these two observations the shear strain is almost entirely recovered upon removal of the applied shear stress. This last observation is important since it demonstrates that all the strains developed are elastic in nature, which is a mandatory requirement of the hollow cylinder methodology. It is also seen that both the axial and tangential strains remain practically zero throughout the entire load–unload cycle. This observation is also indicative of elastic response.

Fig. 9a presents a comparison between the stress–strain response shown in Fig. 8 and that of a second specimen (BGHCB3) brought to failure in torsional shear. The non-linearity of the shear stress–shear strain response is not overwhelming in the plot of Fig. 9a,

Table 1  
Deformation moduli at particular levels of strain

	$\varepsilon = 0^+ \mu\epsilon$	$\varepsilon = 250 \mu\epsilon$	$\varepsilon = 1000 \mu\epsilon$	$\varepsilon = 2000 \mu\epsilon$	$\varepsilon = 4000 \mu\epsilon$
$E'$ (MPa)	2300	2000	1610	1190	900
$E$ (MPa)	4500	3620	2500	2000	1380
$E/E'$	1.95	1.80	1.55	1.65	1.55

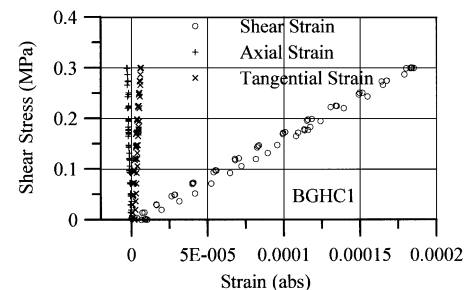


Fig. 8. Stress–strain response during a single loading cycle in torsional shear.

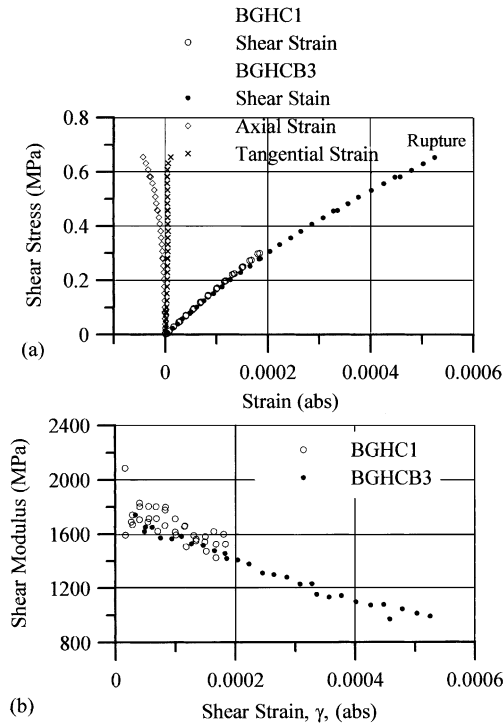


Fig. 9. Results of torsional shear testing: (a) stress–strain response, and (b) variation in shear modulus  $G'$ .

however, it is abundantly clear in Fig. 9b, which plots the shear modulus ( $G'$ ) as a function of the measured shear strain. The initial magnitude of the shear modulus was determined to be 1850 MPa and decreases continuously to a value of 1000 MPa close to failure. No linear zone is apparent. It is also evident that the specimen displayed dilatant behavior as the applied shear stress was increased. The axial strain became increasingly negative (extensile) as the shear stress surpassed 0.4 MPa. The specimen ultimately failed at a shear stress of 0.65 MPa, at a corresponding shear strain ( $\gamma$ ) of  $520 \mu\epsilon$ . Failure of the specimen occurred along a plane oriented at  $40^\circ$  to the horizontal. The normal stress acting across the failure plane was tensile, with a magnitude close to that of the shear stress applied to the  $\theta r$  plane. The shear stress acting upon the failure plane was minimal. It may therefore be concluded that the application of pure shear induced tensile failure in the specimen wall. In line with the response of most rock types, failure in tension is brittle in nature, and occurs following relatively minimal extensile strains.

The results of the uniaxial and radial compressive tests clearly illustrate the differences in moduli of deformation perpendicular and parallel to bedding planes. However, it is not simple to gage the magnitude of the shear modulus as determined by torsional shear of the hollow cylinder specimens. The shear modulus ( $G'$ ) of anisotropic materials is a difficult parameter to quantify. The magnitude of  $G'$  may not be theoretically

determined based on knowledge of the other elastic deformation parameters and therefore, must be measured directly. For instance, had the shear modulus been computed based on the assumption of full isotropy ( $G = E/(2 + 2\nu)$ ) using the elastic parameters determined from uniaxial compression testing, the resulting shear modulus would be 1000 MPa. Talesnick and Ringel [26] demonstrated that use of the commonly accepted empirical relationship (Eq. (4), e.g. [21,32]) for the approximation of  $G'$  of transverse isotropic solids results in significantly lower values than those determined through actual measurement.

$$G' = \frac{E \cdot E'}{E \cdot (1 + 2 \cdot \nu') + E'} \quad (4)$$

Based on typical, initial magnitudes of  $E' = 2300$  MPa,  $E = 4500$  MPa and  $\nu' = 0.15$ , Eq. (4) yields  $G' = 1270$  MPa; only slightly higher than the isotropic prediction and significantly lower than the value of 1850 MPa determined by direct measurement.

#### 4.3. Diametric compression

Fig. 10 presents results of two loading cycles of diametric compression applied to a single Brazilian specimen (BGBraz11). The first loading cycle (open circles) was applied along a diameter coincident with the longitudinal axis of one of the strain gage pairs bonded to the specimen sides (see Fig. 5b). On completion of the first loading cycle the specimen was rotated by  $90^\circ$  and reloaded (solid circles) coincident with the longitudinal axis of the second strain gage pair. The strains measured during the two loading cycles are plotted as a function of the tensile stress at the center of the specimen according to Eq. (3). The fact that the stress–strain responses recorded during the two loading cycles are identical to one another illustrates the mechanically isotropic nature of the material within the plane of the test. Within the context of the present study, this observation strengthens the premise that the horizontal plane of sedimentation is in fact the plane of material isotropy.

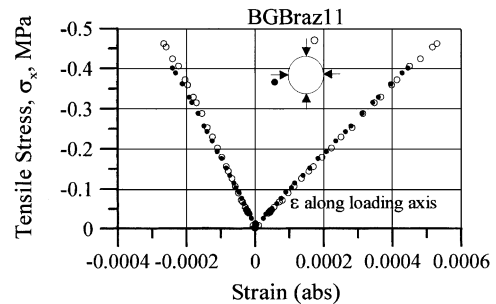


Fig. 10. Stress–strain response to diametric compression in two mutually perpendicular directions.

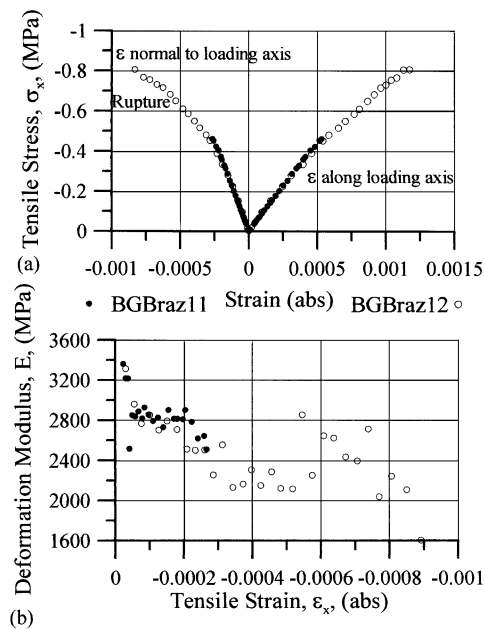


Fig. 11. Results of diametric compression testing: (a) stress–strain response, and (b) variation in modulus of deformation  $E$ .

Fig. 11a presents results of an additional diametric compression test in which the specimen was loaded to failure. In the range of tensile stress up to 0.5 MPa the stress–strain response is the same as that displayed by specimen BGBraz 11. The non-linear response of both specimens is accentuated in Fig. 11b, which plots the variation of the deformation modulus  $E$ , as a function of the measured tensile strain. The figure illustrates the decrease in deformation modulus, from an initial magnitude of 3400 MPa, to a value of less than 2000 MPa at the onset of failure. Failure occurred in diametric splitting when the tensile stresses reached a value of approximately 0.84 MPa, at a tensile strain of  $680 \mu\epsilon$ . Other specimens tested to failure resulted in tensile strengths of 0.95 and 1.04 MPa. These values represent the tensile strength of the chalk in directions parallel to bedding.

The initial modulus of deformation,  $E$  (3400 MPa) based on diametric compression of Brazilian disks is somewhat lower than the value determined from radial compression (4500 MPa), however, it is significantly greater than  $E'$  (2300 MPa) determined from the uniaxial compression tests. A possible explanation for this discrepancy may lie in the fact that the evaluation of  $E$  from the Brazilian test is based on the assumption that the material response to compressive stresses is identical to its response to tensile stresses (see Eq. (5) after [28]).

$$E_{br} = \frac{8 \cdot \sigma_y / \epsilon_x \cdot \sigma_y / \epsilon_y}{9 \cdot \sigma_y / \epsilon_x + 3 \cdot \sigma_y / \epsilon_y}, \quad (5)$$

where the  $y$  direction coincides with the axis of external load.

While this assumption may be very plausible for metals, it is not straightforward for rocks. The stress condition at the center of the Brazilian disk is biaxial,  $\sigma_y$  is compressive and  $\sigma_x$  is tensile (see Fig. 5b). In the situation where the modulus of deformation in tension is less than its compressive counterpart, then  $E_{br}$  determined from Eq. (5) will result in values lower than that representative of the actual compressive response.

#### 4.4. Influence of water content on strength

The effect of water content on the uniaxial compression strength and on the directional dependence of uniaxial compressive strength is illustrated in Fig. 12. The lower set of data plot the uniaxial compressive strength measured perpendicular to bedding as a function of water content. The plot reveals a sharp drop in uniaxial compressive strength due to relatively small increases in water content. For example, the uniaxial compressive strength at a water content of 2% (air-dried condition) is 5.95 MPa; however, at a water content of 5%, the uniaxial compression strength decreases by 20% to a value of 5.0 MPa. As water content increases, the rate of change in uniaxial compressive strength declines, leveling off to a value of 2.8 MPa at “saturated” conditions.

The upper set of data in Fig. 12 represent the compressive strength of the chalk in directions parallel to bedding as a function of water content. This set of results is based on data from radial compression tests. In a fashion similar to that noted for the uniaxial compression strength perpendicular to the bedding, the plot reveals a steep reduction in uniaxial compression

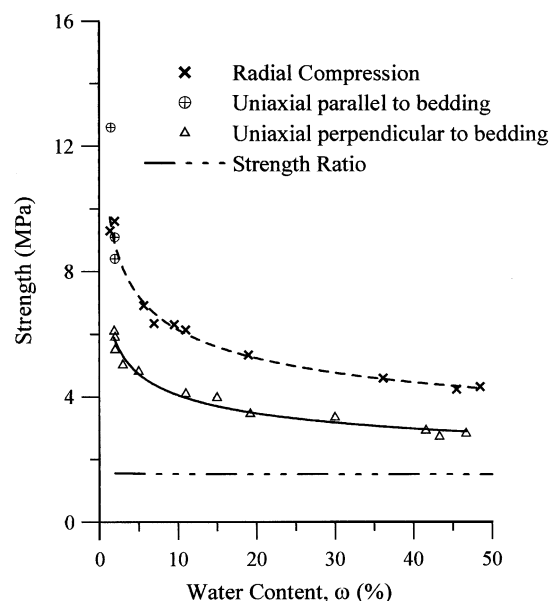


Fig. 12. Variation of compressive strengths as a function of water content.

strength for small changes in water content at low initial water content. The compressive strength decreases by 26% from 9.5 to 7.5 MPa over a change of water content from 2% to 5%. At saturated conditions, the compressive strength parallel to bedding levels off to a value of 4.0 MPa.

Both sets of data are best fitted with power regression curves, as plotted in Fig. 12. The two sets of data demonstrate that the directional dependence of compressive strength is not restricted to the air-dried state and is, in fact, continuous over the entire spectrum of water content. Based on the power curve regressions plotted in Fig. 12, the ratio of the compressive strength parallel to bedding to that perpendicular to bedding may be calculated as a function of water content. The dotted line shown in Fig. 12 is the result of that computation. The ratio of the compressive strength parallel to bedding to that perpendicular to bedding is seen to be almost constant at a value close to 1.5 over the entire range of water contents considered. It is interesting to note that a very similar ratio was found when comparing the deformation modulus parallel and perpendicular to bedding in the air-dry condition.

The effect of variation in water content is not limited to the compressive strength of the chalk. It also greatly reduces the material stiffness. Fig. 13a presents the development of inner tangential strain ( $\epsilon_{\theta i}$ ) recorded

during tests on a set of hollow cylinder specimens in radial compression. The results presented are for specimens with water contents of 1.4%, 5.65% and 36.2%. The plots accentuate two important aspects of the material response. Firstly, as may be expected intuitively, the modulus of deformation ( $E$ ) declines as the water content increases. Secondly, a drastic reduction in modulus of deformation is noted when comparing the response of the specimen tested at air-dried conditions ( $\omega = 1.4\%$ ) to that tested at a water content of 5.65% (Fig. 13b). In fact, the response of the specimen tested at a water content of 5.65% is far more comparable to that of the specimen tested at  $\omega = 36.2\%$  than that tested at  $\omega = 1.4\%$ . The reduction in material stiffness coincides with the drop in compressive strength due to small increases in  $\omega$  at low water contents.

The effect of water content on the tensile strength in directions parallel to the bedding is plotted in Fig. 14. The changes in magnitude in the tensile strength are much smaller than those recorded for the compressive strengths. However, the percentage changes in strength are greater than that of compressive strengths, either parallel or perpendicular to bedding. For example, at a water content of 2% the tensile strength is 0.95 MPa; at a water content of 45% the tensile strength is reduced to 0.3 MPa, a decrease of more than 65%. All specimens failed along sharply defined planes coincident with the loaded diameter. The data in the figure are well fitted by the power regression shown in the plot.

The ratio of compressive strength to tensile strength is often considered in practical engineering situations. The ratio of compressive strength to tensile strength, (within the plane of sedimentation) as a function of water content may be evaluated by dividing the upper power function shown in Fig. 12 by the power function plotted in Fig. 14. The result is shown in Fig. 15. In contrast to the ratio of the compressive strengths plotted in Fig. 12,

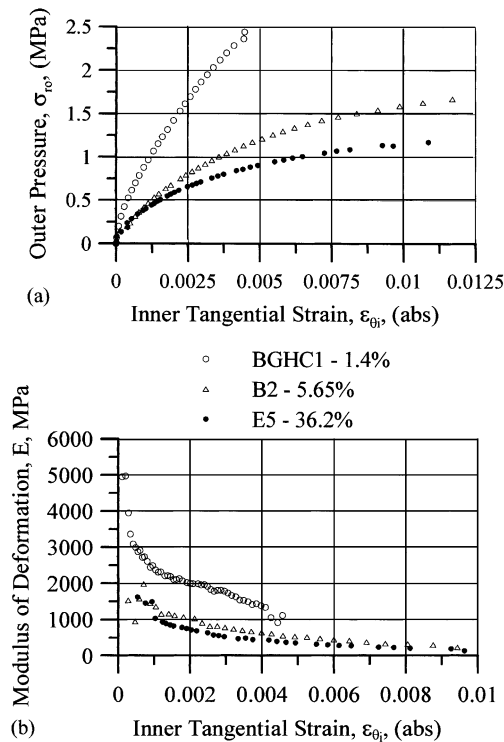


Fig. 13. Effect of water content on results of radial compression testing: (a) stress–strain response, and (b) variation in modulus of deformation,  $E$ .

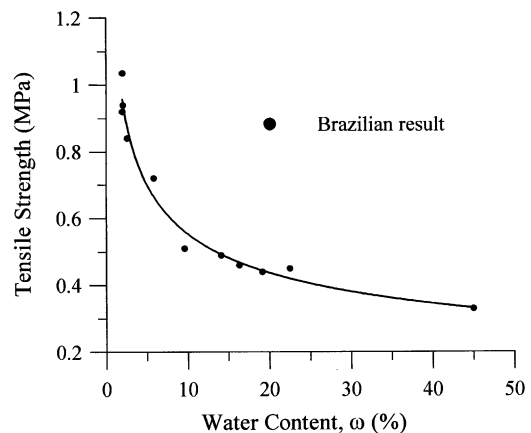


Fig. 14. Variation of tensile strength as a function of water content.

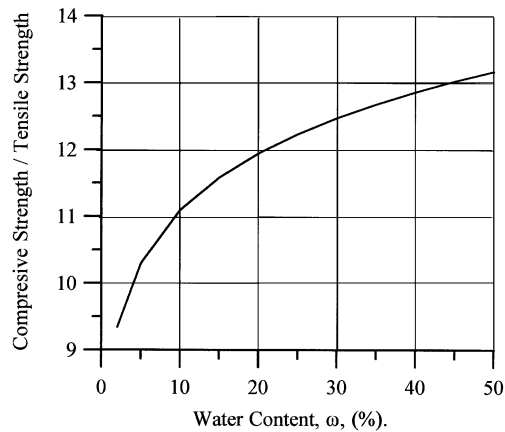


Fig. 15. Ratio of compressive strength to tensile strength parallel to bedding, as a function of water content.

the plot of Fig. 15 illustrates that the tensile strength is reduced to a greater extent than the compressive strength as water content increases. It is interesting to note that at air-dry conditions the ratio between compressive and tensile strengths parallel to bedding is 9.3, which is close to the Griffith value of 8. As water content increases the ratio increases significantly.

## 5. Conclusions

The stress–strain data presented for tests performed on air-dry specimens illustrate the non-linear and anisotropic nature of Marasha chalk. In the four different testing configurations implemented, uniaxial compression, radial compression, hollow cylinder torsion and diametric compression, no linear zone was detected. In fact, the material stiffness declined at a maximum rate upon initial loading. All four testing configurations illustrated the stress–strain anisotropy of the material. The chalk displays transverse isotropy, with the bedding planes defining the plane of material isotropy. The modulus of deformation in directions parallel to bedding planes is 60% higher than that measured perpendicular to bedding. The shear modulus ( $G'$ ) determined from torsional shear tests is significantly higher than that estimated based on isotropic assumptions or accepted empirical relationships.

The anisotropic nature of the chalk was found to be significant in terms of compressive strength. Corroborating results between the different testing schemes lead to the conclusion that the compressive strength in directions parallel to bedding is 50% higher than that measured perpendicular to bedding.

Compressive strengths based on results of radial compression tests on hollow cylinder specimens have been shown to be very compatible to the

uniaxial compressive strength of suitably oriented solid cylinders. This observation reinforces the applicability of the hollow cylinder methodology, which has proven to be a very efficient tool in the study of the stress–strain behavior and strength of this chalk.

The effect of increased water content on the strength of the studied chalk has been addressed. It has been shown that increases in water content significantly reduce the compressive strength of the material. Increases in water content effect strength most dramatically at initially dry conditions. Changes in water content do not influence the anisotropic nature of the material strength. In fact, the ratio of compressive strength within the plane of material isotropy to its counterpart perpendicular to the plane of isotropy is independent of water content. The effect of changes in water content on tensile strength is more pronounced than on compressive strength.

The effect of water content on material stiffness is very pronounced. Drastic reductions in the modulus of deformation are noted due to very mild changes in water content at initially dry conditions.

The physical reason for the sharp changes in stiffness and strength of the chalk due to small changes in water content are currently under consideration. It could be that small changes in water content relieve capillary suctions in the chalk matrix as suggested by Hayati [14] and Mathews and Clayton [18]. Such a condition would result in changes in effective stress, which in turn produce changes in the material strength and response to stress. Two recent failures in overlapping caverns occurred at the start of the rainy season of the winter months.

All of these observations help in understanding the mechanical behavior of the Marasha chalk, and chalks in general, and are essential for rational limit state analysis of underground openings in these chalks. Both the anisotropic nature of the chalk and the effect of changes in water content are currently being integrated into advanced stability analyses of the caverns. Initial results indicate that non-overlapping caverns are not in immediate danger of collapse. The results of these analyses will be forthcoming.

## Acknowledgements

The authors would like to acknowledge the constructive input given by Prof. Sam Frydman in reviewing this manuscript, the financial support of the Israel National Parks Authority, in particular the aid of Engineer Aaron Leviaton and Mr. Yossi Blankstein. The first author acknowledges the financial aid received from the fund for the promotion of research at the Technion.

## References

- [1] Tsesarsky M. Stability of underground openings in jointed chalk—a case study from the bell shaped caverns. M.Sc. Thesis. Beit Guvrin National Park: Ben-Gurion University of the Negev, 1999 (in Hebrew, extended English abstract).
- [2] Tsesarsky M, Hatzor YH, Talesnick ML. The stability of ancient bell shaped caverns at the bet Guvrin National Park—a comprehensive geomechanical study. *Israel J Earth Sci*, 2000;49(2):81–102.
- [3] Kloner A. A guide to the Marasha. Israel antiquities authority, 1996. p. 50 (in Hebrew).
- [4] Loe NM, Leddra MJ, Jones ME. Strain states during stress path testing of chalk. In: Tillerson, Wawersik, editors. Proceedings of the 33rd US Symposium Rock Mechanics, Balkema, 1992. p. 927–36.
- [5] Kageson-Loe NM, Jones ME, Petley DN, Leddra MJ. Fabric evolution during deformation of chalk. *Int J Rock Mech Min Sci Geomech Abstr* 1997;30(7):739–45.
- [6] Addis MA, Jones ME. Mechanical behavior and strain rate dependence of high porosity chalk. Proceedings of the International Chalk Symposium, London: Thomas Telford, 1990. p. 239–44.
- [7] Teufel LW, Rhett DW, Farrell HE. Effect of reservoir depletion and pore pressure drawdown on in-situ stress and deformation in the Ekofisk Field, North Sea. In: Mech R, Roegiers, editors. Proceedings of the 32nd US Symposium, Balkema, 1991. p. 63–72.
- [8] Chin L, Boade RR, Prevost JH, Landa GH. Numerical simulation of shear-induced compaction in the Ekofisk reservoir. *Int J Rock Mech Min Sci Geomech Abstr*. 1993;30(7):1193–200.
- [9] Mortimore RN and Fielding PM. The relationship between texture, density and strength of chalk. Proceedings of the International Chalk Symposium, London: Thomas Telford, 1990. p. 109–32.
- [10] Bell FG, Cripps JC, Edmonds CN and Culshaw MG. Chalk fabric and its relation to certain geotechnical properties. Proceedings of the International Chalk Symposium, London: Thomas Telford, 1990. p. 187–94.
- [11] Clayton, C.R.I. The mechanical properties of the chalk. Proceedings of the International Chalk Symposium, London: Thomas Telford, 1990, p. 213–32.
- [12] Spink TW and Norbury DR. The engineering geological description of chalk. Proceedings of the International Chalk Symposium, London: Thomas Telford, 1990, p. 153–59.
- [13] Kronieger RR. Geotechnical profile of the Maastrichtian chalk. Proceedings of the International Chalk Symposium, London: Thomas Telford, 1990, p. 71–8.
- [14] Hayati G. The engineering geology of some chalks in Israel. D.Sc. Thesis. Technion-Israel Institute of Technology, 1975 (in Hebrew, extended English abstract).
- [15] Flexer A, Honigstein A, Rosenfeld A, Polishook B. Geology, geotechnical properties and exploitation of chalk in Israel—an overview. Proceedings of the International Chalk Symposium, London: Thomas Telford, 1990. p. 63–70.
- [16] Polishook B. Geological and geomechanical qualities of chalk and their application to underground structures. D.Sc. Thesis. Tel Aviv University, 1996 (in Hebrew, extended English abstract).
- [17] Jardine RJ, Brooks NJ, Smith PR. The use of electrolevel gauges in triaxial tests on weak rock. *Int J Rock Mech Min Sci and Geomech Abstr*. 1985;22(5):331–37.
- [18] Matthews MC, Clayton CRI. Influence of intact porosity on the engineering properties of a weak rock. Proceedings of the International Conference on Hard Soils, Soft Rocks, Athens, vol. 1. Rotterdam: Balkema, 1993. p. 693–701.
- [19] Clayton CRI, Gordon MA and Matthews MC. Measurement of stiffness of soils and weak rocks using small strain laboratory testing and field geophysics. Proceedings of the first International Conference on Pre-Failure Deformation Characteristics of Geomaterials, Sapporo, Japan, vol. 1. Rotterdam: Balkema, 1994. p. 229–34.
- [20] Talesnick ML, Brafman M. Small strain deformation characteristics of two chalks subjected to varying stress conditions. *Quart J Eng Geol* 1998;31:161–74.
- [21] Amadei B. Importance of anisotropy when estimating and measuring in situ stresses in rock. *Int J Rock Mech Min Sci* 1996;33(3):293–325.
- [22] Burland JB. Small is beautiful—the stiffness of soils at small strains. *Can Geo J* 1989;26:499–516.
- [23] Jones ME, Leddra MJ, Goldsmith AS, Edwards D. The geomechanical characteristics of reservoirs and reservoir rocks. British, health and safety executive—offshore technology Report OTH 90 333, 1992.
- [24] Bell FG. A note on the physical properties of the chalk. *Eng Geol* 1977;11:217–25.
- [25] Talesnick ML, Lee MY, Haimson BC. On the determination of elastic material parameters for transverse isotropic rocks from a single test specimen. *Rock Mech Rock Eng* 1995;28(1):17–36.
- [26] Talesnick ML, Ringel M. Completing the hollow cylinder methodology for testing of transversely isotropic rocks; Torsion Testing. *Int. J. Rock Mech Min Sci* 1999;39(5):627–39.
- [27] Talesnick ML, Katz A, Ringel M. An investigation of the elastic stress–strain behaviour of a banded sandstone and a sandstone-like material. *ASTM: Geotechnical Testing Journal*, 2000; 23(3):257–73.
- [28] Hondros G. Evaluation of Poissons ratio and modulus of materials of a low tensile resistance the Brazilian (indirect ensile) test with particular reference to concrete. *Australian J Appl Sci* 1959;10:243–68.
- [29] Talesnick ML, Bloch-Friedman EA. Compatibility of different methodologies for the determination of elastic parameters of intact anisotropic rocks. *Int. J. Rock Mech Min Sci* 1999;37(7):919–40.
- [30] Chou PC, Pagano NJ. Elasticity, tensor, dyadic and engineering approaches. New York: Van Nostrand, 1967.
- [31] Santarelli FJ, Brown ET. Failure of three sedimentary rocks in triaxial and hollow cylinder compression tests. *Int. J. Rock Mech Min Sci* 1989;26(5):403–13.
- [32] Itasca. FLAC, version 3.3 User's Manual. Itasca Consulting Group Inc., Minneapolis, Minnesota, 1996.